Nanostructured Tm:CaF$_2$ ceramics: potential gain media for two-micron lasers

F.A. Bol'shchikov, E.A. Garibin, P.E. Gusev, A.A. Demidenko, M.V. Kruglova, M.A. Krutov, A.A. Lyapin, I.A. Mironov, V.V. Osiko, V.M. Reiterov, P.A. Ryabochkina, N.V. Sakharov, A.N. Smirnov, S.N. Ushakov, P.P. Fedorov

Abstract. Tm:CaF$_2$ (4 mol% TmF$_3$) single crystals and ceramic samples have been prepared, the microstructure of the ceramic has been examined by SEM and AFM, and the luminescent properties of the crystals and ceramic have been analysed.

Keywords: single crystals, fluoride ceramics, absorption and luminescence spectra, Tm^{3+} ion, gain cross section.

1. Introduction

Rare-earth-doped ceramic materials are of interest as active laser media [1–3]. The primary reason for this is that, like laser glass, laser ceramics can be scaled to large dimensions and may have high thermal conductivity (comparable to that of single crystals). Moreover, ceramic processing techniques provide a simple way (compared to crystal growth) to produce laser media graded in doping level. In addition, interest in rare-earth-doped ceramics stems from the fact that their luminescence spectra are similar to those of the corresponding single crystals [4, 5].

There has been a considerable research effort devoted to the study of the structure, physical properties and luminescence spectra of oxide laser ceramics doped with various ions, including Nd:YAG ceramics, with the aim of creating diode-pumped high-power solid-state lasers.

There is also undoubted interest in rare-earth-doped fluoride ceramics [6–10] because fluoride materials

(i) have high transmission in a wide spectral range, from 0.16 to 11 μm,

(ii) are easy to dope with rare-earth ions up to a concentration of 10^{21} cm^{-3},

(iii) offer high thermal conductivity and

(iv) possess better mechanical properties and higher moisture resistance in comparison with other substances (chlorides and chalcogenides) that also have a broad transmission window.

A key contribution to the technology of optical fluoride ceramics was made by researchers at the A.M. Prokhorov General Physics Institute, Russian Academy of Sciences, and the Research Institute of Optical Materials Technology, S.I. Vavilov State Optical Institute. They reported the fabrication, structure and mechanical properties of CaF$_2$-based ceramics [7, 8] and the luminescence spectra and lasing properties of Yb:Ca$_{0.6}$Sr$_{0.4}$F$_2$ [9] and Er:CaF$_2$ [10] ceramics.

Considerable attention is currently paid to the search for Tm^{3+}-doped crystalline and ceramic hosts for two-micron lasers for medical and LIDAR applications and for nonlinear optical parametric conversion of light to the mid-IR spectral region. Diode-pumped 2-μm lasing has already been demonstrated in a diversity of Tm^{3+}-doped crystals (Tm:YAG, Tm:YVO$_4$, Tm:YLF, double tungstates and double molybdates) [11–19]. Tunable lasing in this spectral range has also been achieved in Tm:CaF$_2$ single crystals pumped by a Ti:sapphire laser [20]. At the same time, diode-pumped lasing of Tm^{3+}-doped CaF$_2$ crystals or ceramics has not yet been reported, to our knowledge.

The objectives of this work were to prepare CaF$_2$–4 mol% TmF$_3$ (hereafter Tm:CaF$_2$) ceramic samples and to study their microstructure by scanning electron microscopy (SEM) and atomic force microscopy (AFM). We also measured the luminescent properties of the ceramic and Tm:CaF$_2$ single crystals.

2. Sample preparation and characterisation

Tm:CaF$_2$ single crystals were grown by vertical directional solidification (Bridgman method) in an evacuated chamber in graphite crucibles with a graphite resistance heater and graphite thermal shields. Tm:CaF$_2$ ceramic samples were prepared by a severe plastic deformation technique.

The Tm^{3+} concentration in the crystals and ceramic was 9.78×10^{20} cm^{-3}, as determined using the composition dependence of the lattice parameter for solid solutions of thulium fluoride in fluorite, Ca$_{1-x}$Tm$_x$F$_{2+x}$: $a = 5.463 + 0.144x$.

The microstructure of the Tm:CaF$_2$ ceramic was examined on a μVizo-103 optical microscope after etching with concentrated sulphuric acid. The ceramic was also characterised by SEM on a JEOL JSM-6490.

The surface morphology of the ceramic samples was imaged by AFM with a Solver Pro instrument (NT-MDT, Zelenograd, Russia). AFM images were obtained under atmospheric conditions in contact mode using NT-MDT NSG-11 rectangular silicon cantilever probes with a tip curvature radius $R < 10$ nm (manufacturer's data). The lateral resolution in

F.A. Bol'shchikov, A.A. Lyapin, P.A. Ryabochkina N.P. Ogarev Mordovian State University, Bol'shevistkaya ul. 68, 430005 Saransk, Russia; e-mail: ryabochkina@freemail.mrsu.ru;
M.V. Kruglova, N.V. Sakharov N.I. Lobachevsky Nizhnii Novgorod State University, prosp. Gagarina 23, 603950 Nizhnii Novgorod, Russia; e-mail: nvsakharov@nifti.unn.ru;
V.V. Osiko, S.N. Ushakov, P.P. Fedorov A.M. Prokhorov General Physics Institute, Russian Academy of Sciences, ul. Vavilova 38, 119991 Moscow, Russia; e-mail: userg@mail15.com;
E.A. Garibin, P.E. Gusev, A.A. Demidenko, M.A. Krutov, I.A. Mironov, V.M. Reiterov, A.N. Smirnov INCROM Ltd., ul. Babushkina 36, 193171 St. Petersburg, Russia

our AFM measurements was down to 10 nm, and the vertical resolution was down to 1 nm. AFM results were analysed using application software: SZM NT-MDT Nova Image Analysis 2.0 and SPMLab Analysis Only 5.01 (Veeco Instruments, USA).

Luminescence spectra of the Tm:CaF$_2$ single crystals and ceramic were measured using an automatic system built around an MDR-23 monochromator. Absorption spectra were obtained using a halogen lamp as a light source. Luminescence was excited by an 800-nm laser diode and was detected using an FEU-100 photomultiplier, FD-7G germanium photodiode or PbS photoresistor, depending on the spectral range.

3. Experimental results

Figure 1 shows micrographs of Tm:CaF$_2$ ceramic samples at two different magnifications. Analysis of micrographs of etched samples indicates that the grains have a hierarchical structure. There are very large grains, about 1 mm in size. Their boundaries are the first to be revealed by etching. Sufficiently long etches demonstrate that the large grains are composed of finer grains, 30–50 μm in size. As shown by Akchurin et al. [8], the grains in CaF$_2$-based ceramics typically have a nanotwinned structure. To verify whether or not the Tm:CaF$_2$ ceramic samples had such a nanostructure, they were examined by SEM and AFM.
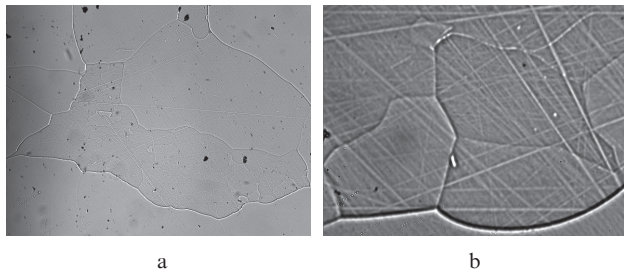
Figure 1. Micrographs of Tm:CaF$_2$ ceramic samples at magnifications of (a) 5$^\times$ and (b) 100$^\times$.

Figure 2 shows SEM micrographs of a fracture surface of the Tm:CaF$_2$ ceramic. The fracture surface is seen to have the form of a set of parallel lamellae 0.3 to 0.5 μm thick. In AFM images of the Tm:CaF$_2$ ceramic (Fig. 3), a fine layered structure is well seen. At higher magnifications, the fracture surface is seen to consist of lamellae 50 to 250 nm thick. From surface profiles in sections normal to the layer direction, the average layer height was estimated at 5–10 nm (Fig. 4). Note that the SEM and AFM results for the Tm:CaF$_2$ ceramic correlate
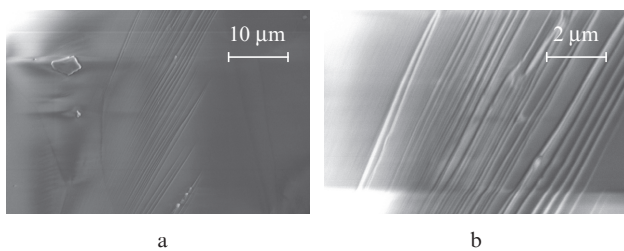
Figure 2. SEM micrographs of a fracture surface of the Tm:CaF$_2$ ceramic: (a) general appearance, (b) higher magnification.
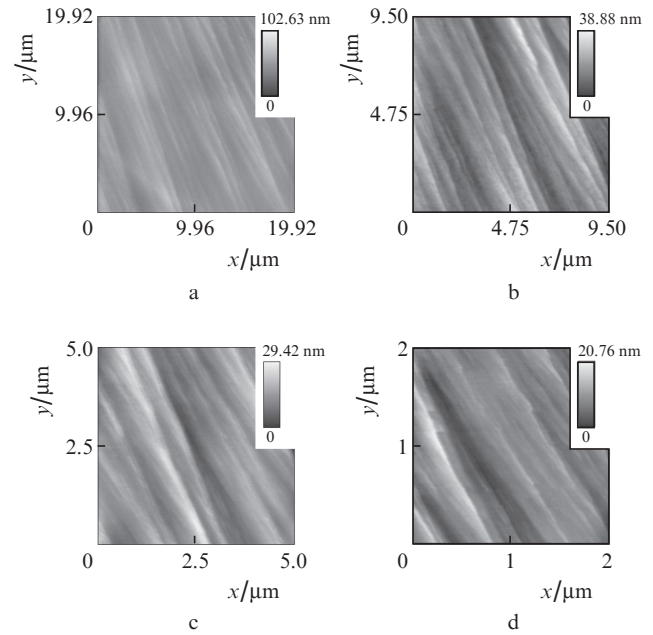
Figure 3. AFM images of a fracture surface of the Tm:CaF$_2$ ceramic at different magnifications.
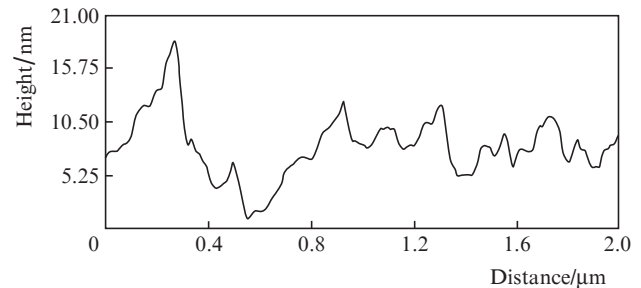
Figure 4. Surface profile in a section normal to the layer direction in a Tm:CaF$_2$ ceramic sample.

with those reported earlier for CaF$_2$, Nd:CaF$_2$ and Yb:CaF$_2$ ceramics [8].

Figure 5 presents the 300-K absorption spectra of the Tm^{3+} ion in the Tm:CaF$_2$ crystals and ceramic. The absorptions are due to the transitions from the $^3H_6$ ground state to the $^1G_4$, $^3F_2$, $^3F_3$, $^3H_4$ and $^3H_5$ excited multiplets. The spectra of the Tm:CaF$_2$ crystals are similar in shape to those reported by Doualan et al. [21]. The peak absorption cross sections obtained for the $^3H_6 \rightarrow {}^3H_4$ transition in this study and in Ref. [21] coincide to within the precision of the measurements.

It follows from Fig. 5 that the absorption spectra of the crystals and ceramic are essentially identical. At the same time, the $^3H_6 \rightarrow {}^3H_4$ absorption peak in the spectra of the Tm:CaF$_2$ crystals and ceramic is shifted to shorter wavelengths in comparison with oxide crystals.

A key characteristic of a gain medium is the gain cross section of the laser transition, σ_g. To obtain the $\sigma_g(\lambda)$ of the $^3F_4 \rightarrow {}^3H_6$ transition in the Tm:CaF$_2$ crystals and ceramic, we determined the spectral dependence of the luminescence cross section, $\sigma_{em}(\lambda)$, for this transition using the Fuechtbauer–Ladenburg formula:
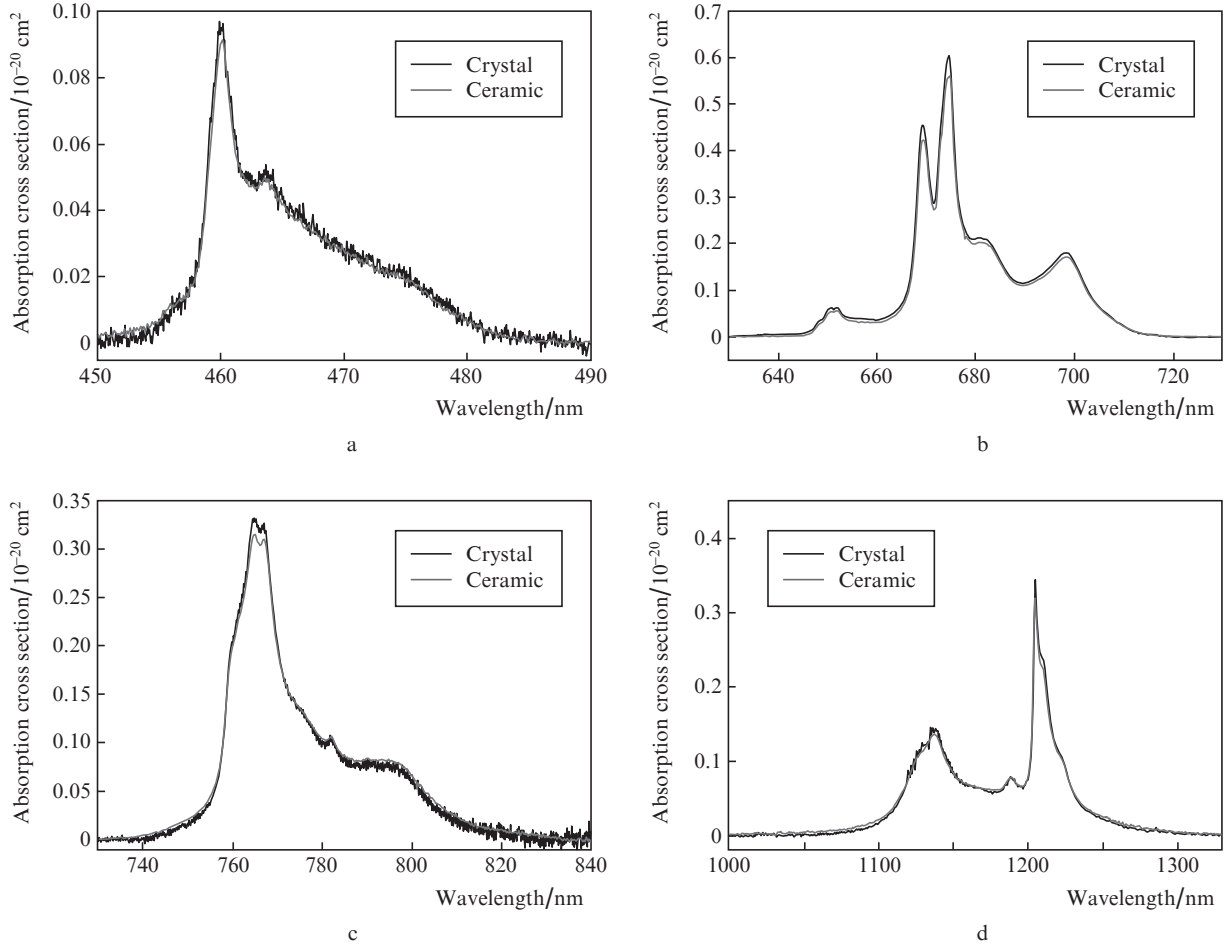
Figure 5. 300-K absorption spectra of the Tm:CaF$_2$ crystals and ceramic: (a) $^3H_6 \rightarrow {}^1G_4$, (b) $^3H_6 \rightarrow {}^3F_2 + {}^3F_3$, (c) $^3H_6 \rightarrow {}^3H_4$ and (d) $^3H_6 \rightarrow {}^3H_5$ transitions.

$$\sigma_{em}(\lambda) = \frac{\lambda^5 \beta_{JJ'} I_{em}(\lambda)}{8\pi c n^2 \tau_{rad}\left(\int I_{em}(\lambda)\lambda\,d\lambda\right)}, \qquad (1)$$

where τ_{rad} is the radiative lifetime of Tm^{3+} at the $^3F_4$ level; n is the refractive index of the medium ($n = 1.42$ in CaF$_2$ crystals and ceramics); $I_{em}(\lambda)$ is the relative luminescence intensity; c is the speed of light; and $\beta_{JJ'}$ is the fluorescence branching ratio ($\beta_{JJ'} = 1$ for the $^3F_4 \rightarrow {}^3H_6$ transition). Assuming that the probability of nonradiative decay from the $^3F_4$ level is low, we used $\tau_{rad} = A^{-1} = 14.2$ ms. Here, A is the probability of a radiative transition from the $^3F_4$ level, which was evaluated as

$$A = \frac{8\pi c n^2}{n_0 \lambda^4} \frac{2J'+1}{2J+1}\int k(\lambda)\,d\lambda, \qquad (2)$$

where n_0 is the Tm^{3+} concentration; $k(\lambda)$ is the absorption coefficient; and J' and J are the total angular momentum quantum numbers of the 4f electrons in the ground state and the excited state involved in the transition.

$^3F_4 \rightarrow {}^3H_6$ luminescence spectra were measured under excitation with an 800-nm laser diode and were corrected using coefficients obtained by calibrating the measuring system against a certified TRSh 1045-2200 reference lamp. The

spectral dependences of the absorption cross section $\sigma_{abs}(\lambda)$ and luminescence cross section $\sigma_{em}(\lambda)$ for the $^3H_6 \rightarrow {}^3F_4$ transition at 300 K are presented in Fig. 6.

From the absorption and luminescence spectra, we derived the spectral dependence of the gain cross section, $\sigma_g(\lambda)$, for the assumed $^3F_4 \rightarrow {}^3H_6$ laser transition:

$$\sigma_g(\lambda) = P\sigma_{em}(\lambda) - (1-P)\sigma_{abs}(\lambda), \qquad (3)$$

where P is the relative inverted population of the levels involved.

Figure 7 shows the $\sigma_g(\lambda)$ curves for $P = 0.4$, 0.5 and 0.6. It follows from these data that the gain band of the Tm:CaF$_2$ crystals and ceramic extends from 1700 to 2000 nm.

4. Conclusions

Tm^{3+}-doped CaF$_2$ ceramic samples have been studied by optical spectroscopy, SEM and AFM, and the luminescent propertiesof the ceramic and Tm:CaF$_2$ single crystals have been measured. The results demonstrate that the $^3H_6 \rightarrow {}^1G_4$, $^3F_2 + {}^3F_3$, $^3H_4$, $^3H_5$ and $^3F_4$ absorption bands and the $^3F_4 \rightarrow {}^3H_6$ luminescence band in the ceramic are similar in shape to those in the crystals. We have estimated the shape of the gain band for the two-micron laser transition $^3F_4 \rightarrow {}^3H_6$ at different relative inverted population parameters. The gain band of the crystals and ceramic extends from 1700 to 2000 nm.
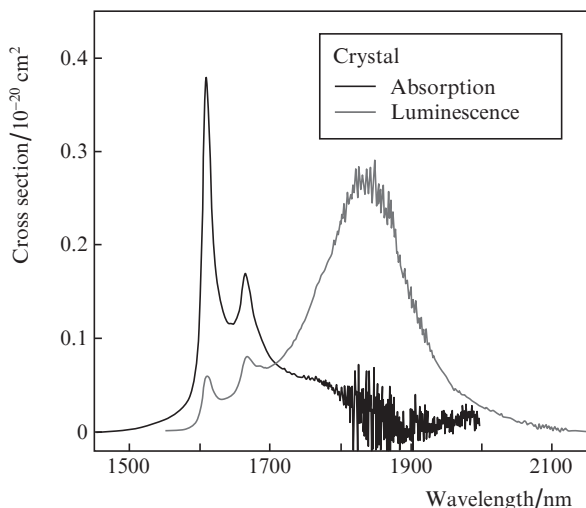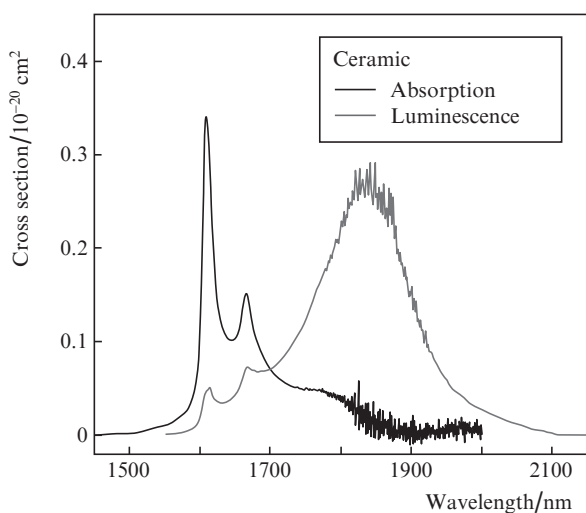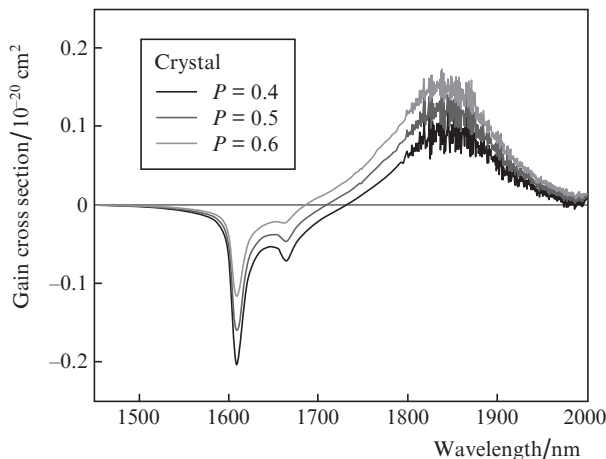
Figure 6. 300-K absorption and luminescence spectra of the Tm:CaF$_2$ (a) crystals and (b) ceramic for the $^3H_6 \rightarrow {}^3F_4$ transition.
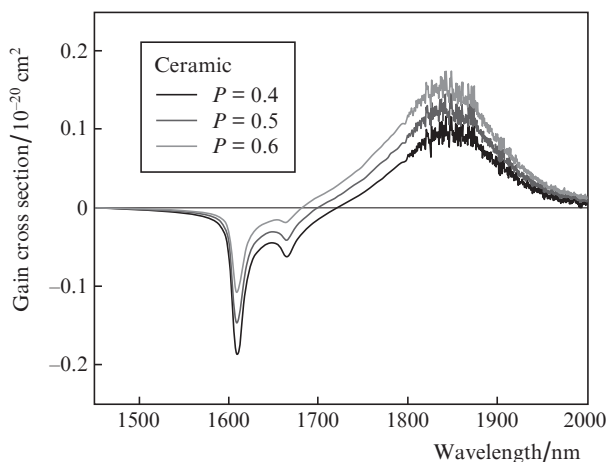
References

1. Ikesue A., Kinoshita T., Kmata K., Yoshida K. *J. Am. Ceram. Soc.*, **78**. 1033 (1995).
2. Lu J.R., Lu J.H., Murai T., Uematsu T., Shirakava A., Ueda K., Yagi H., Yanagitani T., Kaminskii A.A. *Jpn. J. Appl. Phys. Lett.*, **40** (12A), L1277 (2001).
3. Takaichi K., Lu J.R., Murai T., Uematsu T., Shirakawa A., Ueda K., Yagi H., Yanagitani T., Kaminski A.A. *Jpn. J. Appl. Phys. Lett.*, **41** (2A), L96 (2002).
4. Bagaev S.N., Osipov V.V., Ivanov V.I., Solomonov V.I., Platonov V.V., Orlov A.N., Rasuleva A.V., Ivanov V.V., Kaigorodov A.S., Khrustov V.R., Vatnik S.M., Vedin I.A., Maiorov A.P., Pestryakov E.V., Shestakov E.V., Salkov A.V. *Kvantovaya Elektron.*, **38** (9), 840 (2008) [*Quantum Electron.*, **38** (9), 840 (2008)].
5. Kaminski A.A., Kravchenko V.B., Kolupov Yu. L., Bagaev S.N., Shemet V.V., Komarov A.A., Kallmeyer F., Eichler H.J. *Phys. Status Solidi A*, **204** (7), 2411 (2007).

Figure 7. Spectral dependences of the $^3F_4 \rightarrow {}^3H_6$ gain cross section $\sigma_g(\lambda)$ for the Tm:CaF$_2$ (a) crystals and (b) ceramic.

6. Akchurin M.Sh., Gainutdinov R.V., Smolyanskii P.L., et al. *Dokl. Akad. Nauk*, **406** (2), 180 (2006).
7. Fedorov P.P., Osiko V.V., Basiev T.T., Orlovskii Yu.V., Dukel'skii K.V., Mironov I.A., Demidenko V.A., Smirnov A.N. *Ross. Nanotekhnol.*, **2** (5-6), 95 (2007).
8. Akchurin M.Sh., Gainutdinov R.V., Garibin E.A., Golovin Yu.I., Demidenko A.A., Dukel'skii K.V., Kuznetsov S.V., Mironov I.A., Osiko V.V., Smirnov A.N., Tabachkova N.Yu., Tyurin A.I., Fedorov P.P., Shindyapin V.V. *Perspekt. Mater.*, **5**, 1 (2010).
9. Basiev T.T., Doroshenko M.E., Fedorov P.P., Konyushkin V.A., Kouznetsov S.V., Voronov V.V., Osiko V.V., Akchurin M.Sh. *Opt. Lett.*, **33** (5), 521 (2008).
10. Basiev T.T., Orlovskii Yu.V., Polyachenkova M.V., Fedorov P.P., Kuznetsov S.V., Konyushkin V.A., Osiko V.V., Alimov O.K., Dergachev A.Yu. *Kvantovaya Elektron.*, **36** (7), 591 (2006) [*Quantum Electron.*, **36** (7), 591 (2006)].
11. Suni J.M., Henderson S.W. *Opt. Lett.*, **16** (11), 817 (1991).
12. Stoneman R.C., Esterowitz L. *Opt. Lett.*, **15** (9), 486 (1990).
13. Honea E.C., Beach R.J., Sutton S.B., Speth J.A., Mitchell S.C., Skidmore J.A., Emanuel M.A., Payne S.A. *IEEE J. Quantum Electron.*, **33** (9), 1592 (1997).
14. Zayhowski J.J., Harrison J., Dill C., Ochou J. *Appl. Opt.*, **34** (3), 435 (1995).
15. Budni D.A., Lemons M.L., Mosto J.R., Chicklis E.P. *IEEE J. Sel. Top. Quantum Electron.*, **6**, 629 (2000).
16. Cano-Torres M., Han X., Garcia-Cortes A., Serrano M.D., Zaldo C., Valle F.J., Mateos X., Rivier S., Rico M., Griebner U., Petrov V. *Mater. Sci. Eng. B*, **146**, 22 (2008).

17. Cano-Torres J.M., Serrano M.D., Zaldo C., Rico M., Mateos X., Liu J., Griebner U., Petrov V., Valle F.J., Galan M., Viera G. *J. Opt. Soc. Am. B*, **23** (12), 2494 (2006).
18. Bol'shchikov F.A., Zharikov E.V., Zakharov N.G., Lis D.A., Ryabochkina P.A., Subbotin K.A., Antipov O.L. *Kvantovaya Elektron.*, **40** (2), 101 (2010) [*Quantum Electron.*, **40** (2), 101 (2010)].
19. Bol'shchikov F.A., Zharikov E.V., Lis D.A., Zakharov N.G., Ryabochkina P.A., Subbotin K.A., Antipov O.L. *Kvantovaya Elektron.*, **40** (10), 847 (2010) [*Quantum Electron.*, **40** (10), 847 (2010)].
20. Camy P., Doualan J.L., Renard S., Braud A., Ménard V., Moncorgé R. *Opt. Commun.*, **236** (4-6), 395 (2004).
21. Doualan J.L., Gamy P., Moncorge R., Daran E., Couchland M., Ferrand B. *J. Fluorine Chem.*, **128**, 459 (2007).